



Originally published as:

Zhu, Y., Vieth-Hillebrand, A., Wilke, F., Horsfield, B. (2015): Characterization of water-soluble organic compounds released from black shales and coals. - *International Journal of Coal Geology*, 150-151, p. 265-275.

DOI: <http://doi.org/10.1016/j.coal.2015.09.009>

1 Characterization of water-soluble organic compounds released from black shales and coals

2 Yaling Zhu, Andrea Vieth-Hillebrand, Franziska D.H. Wilke, Brian Horsfield

3 Helmholtz Centre Potsdam, GFZ German Research Centre for Geosciences, Telegrafenberg, D-14473 Potsdam, Germany

4 **Abstract:** Knowledge of the composition of dissolved organic compounds as well as the main controls
5 on their mobilization from natural organic matter is prerequisite for a comprehensive understanding of
6 the fluid-rock interactions taking place in shale environments and coal seams over both geological and
7 human timescales. In this study, black shales and coals from five different geological settings and
8 covering the maturity range $R_o = 0.3 - 2.6\%$ were extracted with deionized water. The dissolved
9 organic carbon (DOC) yields were found to decrease rapidly with increasing diagenesis and remain
10 low throughout catagenesis. Four different fractions of DOC have been qualitatively and quantitatively
11 characterized in the study using size exclusion chromatography (SEC). Acetate is the dominant low
12 molecular weight organic acid (LMWOA) in all extracts of shales and coals of bituminous rank. The
13 concentrations of individual LMWOA also decrease with increasing maturity of the samples except
14 for acetate extracted from the overmature Posidonia shale from the Haddessen well, which was
15 influenced by hydrothermal brines. The positive correlation between the Oxygen Index (OI) and
16 respective LMWOA yield indicates that OI is a significant factor influencing the extraction of organic
17 acids from shales. The yields of both DOC and individual organic acids normalized to TOC are in the
18 same order of magnitude for coals and shales with the same maturity. However, the extracts of coals
19 tend to contain more aromatic compounds and the molecular masses of most constituents included in
20 macromolecular fractions are higher than for shale extracts. These results suggested that different
21 kerogen types show comparable amounts of DOC being extracted, but different DOC composition.
22 Thus, both the origin of organic matter and thermal maturation progress during deposition has
23 significant influence on water extract composition.

24 Key words: Dissolved organic carbon; Low molecular weight organic acids; Maturity; Size-exclusion
25 chromatography; Shales; Coals

26 **Highlights:**

- 27 • Maturity of samples affects the concentration of DOC in water extracts.
- 28 • Composition of dissolved organic matter is influenced by the kerogen types.
- 29 • Acetate is the dominant LMWOAs in the water extracts of shale samples.
- 30 • The concentration of LMWOAs in extracts is constrained by OI of shales and coals.
- 31 • Hydrothermal processes might enhance the generation of acetate.

32 **1. Introduction**

33 Dissolved organic carbon (DOC) is defined as the fraction of organic matter in water that passes
34 through a filter with pore size $0.45\mu\text{m}$ (Herbert and Bertsch, 1995). DOC in near-surface groundwater
35 and natural formation waters like oil field brines has been studied for years (Leenheer and Croué, 2003;
36 Lepane et al., 2004; Schmidt et al., 2009) and the first insights into the molecular composition have
37 been provided. Special attention has been paid to the abundance and origin of low molecular weight
38 organic acids (LMWOAs) in subsurface brines (Means and Hubbard, 1987). LMWOAs have been
39 proposed as tracers or proximity indicators of hydrocarbons (Zinger and Kravchik, 1973), and
40 Kharaka et al. (1983) argued that acid anions are important precursors of natural gas via thermal
41 cracking. LMWOAs are assumed to create secondary porosity in the subsurface by increasing the
42 dissolution of aluminosilicates and carbonates (Surdam et al., 1984). Additionally, LMWOAs can act
43 as feedstock for the deep terrestrial biosphere (Horsfield et al., 2006; Vieth et al., 2008). As far as oil
44 and gas production is concerned, it has been reported that LMWOAs make up a dominant fraction of
45 DOC in waters utilized during oil shale retorting (Dobson et al., 1985; Leenheer et al., 1982). High
46 concentrations of formate and acetate in flowback waters were previously reported in fracturing
47 flowback (Lester et al., 2015; Olsson et al., 2013). The amount and composition of other organic
48 compounds in flowback and produced waters from hydraulic fracturing of shales have been reported in
49 recent years (Maguire-Boyle and Barron, 2014; Orem et al., 2014). Although the occurrence of DOC
50 and LMWOAs in different types of natural waters is well documented, only little work has been done
51 to elucidate the relation between their quantitative and qualitative occurrence in water and the
52 properties of the rock they have been in contact with.

53 Black shales and coals usually contain high concentrations of organic matter. During progressive
54 burial over geological times, reactive functional groups within the organic material are thermally
55 degraded. It is well known that during diagenesis, with vitrinite reflectance (R_o) below 0.5%,
56 biopolymers such as polysaccharides, proteins and amino sugars are initially degraded by
57 microorganisms in the water column and in young sediments, after which a loss of hydrolysable
58 moieties takes place during continuing subsidence (Tissot and Welte, 1984). Catagenesis ($R_o = 0.5 -$

59 2.0%) is characterized by the progressive cracking of carbon-carbon and carbon-oxygen bonds
60 accompanied by aromatization and condensation of the kerogen (Kelemen et al., 2007; Lis et al., 2005;
61 Petersen et al., 2008; Robin and Rouxhet, 1978; Werner-Zwanziger et al., 2005). The generation of
62 LMWOAs in sedimentary basins has been attributed to the cleavage of kerogen fragments containing
63 carboxylic functional groups during the early stage of thermal maturation (Cooles et al., 1987).
64 Decreasing yields of ester-bound LMWOA generated with increasing maturity of coals has been
65 reported (Glombitza et al., 2009). In addition, oxidation reactions involving mineral oxidants may also
66 produce organic acids during thermal maturation (Borgund and Barth, 1994; Seewald, 2001a, b;
67 Surdam et al., 1993).

68 Knowing the composition, molecular size and structure of the DOC as well as the main controls on the
69 release of DOC are prerequisites for a better understanding of the fluid-rock interactions taking place
70 in shale environments over both geological and human timescales. Soxhlet extraction of marine
71 sediments accesses a larger and more complex pool of organic matter than that contained in interstitial
72 pore water (Schmidt et al., 2014). Hot water extraction of organic matter has also been previously
73 applied to soils to examine the labile organic fractions (Bu et al., 2010; Ghani et al., 2003; Gregorich
74 et al., 2003; Sarkhot et al., 2011). Thus, water extraction is an appropriate tool for studying the soluble
75 organic matter released during the interaction between water and rock. As far as we are aware,
76 leaching experiments have only rarely been applied to black shales and coals (Bou-Raad et al., 2000;
77 Vieth et al., 2008) and little attention has been paid to how DOC composition varies as a function of
78 organofacies, organic matter type and maturity. In the present contribution, we report the composition
79 of DOC in water extracts from shales and coals not only of different geological ages and depositional
80 settings, thereby covering different kerogen types, but also different thermal maturation levels,
81 enabling the controls of progressive thermal maturation on composition of water extracts to be
82 documented.

83 **2. Materials**

84 Thirty-two organic-rich black shales and coals from around the world, representing a wide range of
85 depositional settings and ages (Paleozoic through Cenozoic age) were selected for this study (Table 1).

86 The samples cover a maturity range from immature ($R_o = 0.29$; $T_{max} = 409^\circ\text{C}$) to overmature ($R_o = 2.6$;
87 $T_{max} = 602^\circ\text{C}$) with TOC contents of shales and coals extending up to 15% and 67%, respectively. The
88 chain length distribution of *n*-alkyl moieties (C_{1-5} total, *n*- C_{6-14} , *n*- C_{15+}) in pyrolysates of the original
89 samples is illustrated in the ternary diagram of Horsfield (1989) (Fig. 1). The pyrolysate compositions
90 of shale samples indicate Paraffinic-Naphthenic-Aromatic Low Wax Oil petroleum type as well as Gas
91 and Condensate petroleum type organofacies. The chain length distributions of the macromolecular
92 organic matter in shale samples are closely similar despite their diverse origins. The three bituminous
93 coals (C3, C4 and C5) fall in the High Wax, Paraffinic-Naphthenic-Aromatic Oil petroleum type and
94 the two lignites C1 and C2 fall in Paraffinic Oil High Wax organofacies. Relative percentages of the
95 three main minerals of the shale samples are shown in Fig. 2. The Posidonia and Duvernay shales are
96 dominated by carbonate, whereas the Bakken and Alum shales are characterized by higher contents of
97 quartz and clays, respectively.

98 2.1 Posidonia shale

99 The Lower Toarcian Posidonia shale samples are from three shallow boreholes (Wickensen,
100 Harderode, Haddessen) located in the Hils Syncline of Northwest Germany and cover a large maturity
101 range from immature to overmature (Rullkötter et al., 1988). The shale was deposited in a restricted
102 epicontinental sea with prevailing anoxic conditions, and the organic matter originates mostly from
103 marine phytoplankton with minor terrigenous input (Littke et al., 1991). Comprehensive studies on the
104 Posidonia shales have been presented by several authors, on nanoscale structure (Bernard et al., 2010;
105 Bernard et al., 2012), petrophysical characteristics (Mann and Müller, 1988) and biogeochemistry
106 (Wilkes et al., 1998). The depositional conditions and the preservation of organic matter are
107 considered to be uniform for the three sampling sites (Littke et al., 1988; Littke et al., 1991; Rullkötter
108 et al., 1988).

109 2.2 Bakken shale

110 The Devonian-Mississippian Bakken shale samples from six wells located in the Williston Basin in
111 North Dakota, USA and covering the immature to mature range, were supplied by the North Dakota

112 Geological Survey. The Bakken shale was deposited in an epicontinental setting (Jiang et al., 2001)
113 under anoxic and uniformly quiet conditions, judging by the widespread occurrence of planar and thin
114 laminations (Webster, 1984). Amorphous organic matter derived from marine algae dominates, and
115 terrestrial contributions are minor (Smith and Bustin, 1998). The detailed petroleum system has been
116 investigated in previous studies (Jiang and Li, 2002; Kuhn et al., 2010; Kuhn et al., 2012; Leenheer,
117 1984; Muscio et al., 1994).

118 2.3 Duvernay shale

119 Six samples were taken from the Upper Devonian Duvernay Formation in the Western Canada
120 Sedimentary Basin, and supplied by the Geological Survey of Canada. They follow a progressive trend
121 in maturity from northeast to southwest. Two principal interbedded lithofacies are present: the nodular
122 to nodular-banded lime mudstones exhibit varying degrees of bioturbation and indicate relatively
123 oxygenated conditions; the dark bituminous laminated lime mudstones were deposited in deep water
124 under oxygen-starved conditions (Chow et al., 1995; Creaney and Allan, 1990; Dieckmann et al., 2004;
125 Li et al., 1997). The organic matter is mainly of marine planktonic origin as indicated by, for example,
126 the biomarker value of pristane/*n*-C₁₇ versus phytane/*n*-C₁₈ (Li et al., 1997) and petrographic
127 composition (Dieckmann, 1999).

128 2.4 Alum shale

129 The Alum shale samples were collected from a shallow well located in the south of the island of
130 Bornholm, Denmark, which covers stratigraphic ages from Middle Cambrian to Lower Ordovician
131 (Schovsbo et al., 2011). The shale formation is considered to have been deposited in a predominantly
132 anoxic marine environment as the TOC content of the Alum shale is very high (Buchardt et al., 1986;
133 Buchardt and Lewan, 1990). The Alum shale comprises homogeneous fine-grained mudstone and a
134 low proportion of limestone occurring as beds and nodules, which indicate a uniform depositional
135 environment (Buchardt et al., 1986). All the Alum shale samples, having evolved from an alginite-rich
136 Type II kerogen (Horsfield et al., 1992), have a very high thermal maturity with the reflectance of
137 “vitrinite-like” particles being about 2.3% (Buchardt and Lewan, 1990).

138 2.5 New Zealand coal

139 The Cenozoic coal samples were gathered from one drilled core and two coal mines in New Zealand.
 140 Three samples were taken from the DEBITS-1 well located in the Waikato Coalfield, two of which
 141 were lignites from above an unconformity and one of sub-bituminous rank from below the
 142 unconformity (Kallmeyer et al., 2006). The sample from Rotowaro Mine in Waikato Basin represents
 143 sub-bituminous coal and the one from Welcome Mine in West Coast Basin is a coal of High Volatile
 144 Bituminous rank (Vu et al., 2009).

145 Table 1: Sample origin and Rock-Eval pyrolysis characteristics. Hydrogen Index (HI) and Oxygen Index (OI)
 146 are measured in mg hydrocarbons/g organic carbon and mg CO₂/g organic carbon, respectively. TOC and Rock-
 147 Eval data of Duvernay shales and New Zealand coals were taken from (Dieckmann, 1999) and Glombitza (2011),
 148 respectively. Posidonia, Bakken and Alum shale samples were analyzed in this study. Ro values of Posidonia,
 149 Bakken, Alum and New Zealand samples were taken from Rullkötter et al. (1988), Dembicki and Pirkle (1985),
 150 Buchardt and Lewan (1990), and Glombitza (2011) respectively. Ro of Duvernay shales was calculated using the
 151 empirical formula %Ro = 0.018 * T_{max} - 7.16 (%) (Jarvie et al., 2007).

ID	Well	Depth (m)	TOC (%)	Tmax (°C)	OI	HI	Ro (%)
<i>(A) Black shale, Posidonia Formation, Germany, Lower Jurassic, Type II</i>							
P1	Wickensen	58.2	9.9	430	14	664	0.53
P2*	Wickensen	42.2	9.0	432	16	658	0.53
P3	Wickensen	30.2	11.4	433	14	634	0.53
P4	Harderode	77.3	4.8	447	7	340	0.88
P5*	Harderode	42.5	7.2	449	7	384	0.88
P6	Harderode	55.7	11.0	449	5	282	0.88
P7	Haddessen	36.6	9.2	466	9	87	1.45
P8*	Haddessen	51.0	5.0	466	16	79	1.45
P9	Haddessen	60.6	7.7	469	8	66	1.45
<i>(B) Black shale, Bakken Formation, USA, Mississippian, Type II</i>							
B1*	Daniel Anderson 1	1012.1	9.4	409	28	360	0.35
B2	Dobrinski 18-44	2631.7	14.9	423	12	420	0.45
B3	Nordstog 14-23-161-98H	2651.6	12.1	440	3	462	0.7
B4	Loucks 44-30	2350.8	15.0	440	2	460	0.75
B5*	Titan E-Gierke 20-1-H	3351.6	11.9	452	3	118	0.86
B6	BR 12-29	3253.7	8.4	452	4	93	1.1
<i>(C) Black shale, Duvernay formation, Canada, Late Devonian, Type II</i>							
D1*	Sarcee et al Pibroc	1395.9	6.4	418	19	619	0.36
D2	Imperial Kingman	1404.2	2.4	427	32	412	0.53

D3	Bangg Imperial	1677.9	5.5	431	6	621	0,6
D4	Tomahawk	2337.5	4.8	435	7	620	0.67
D5*	Imperial Cynthia	2976.1	1.9	447	12	92	0.89
D6*	Banff Aguit Ram River	4623.9	2.0	542	17	4	2.6

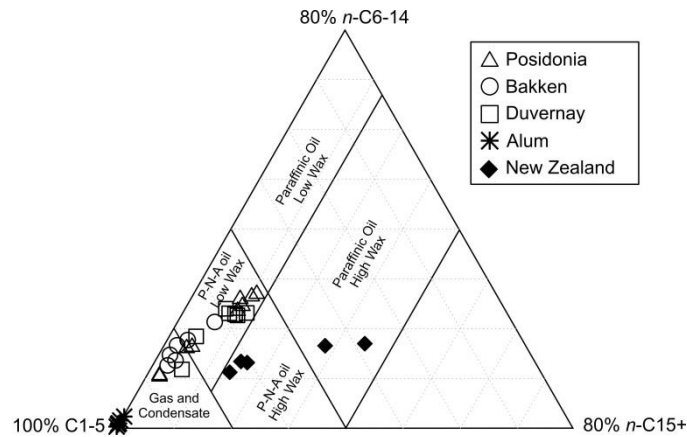
(D) Black shale, Alum Formation, Denmark, Lower Ordovician to Middle Cambrian, Type II

A1	Skelbro-2	39.6	6.3	564	2	3	2.3
A2*	Skelbro-2	27.0	10.1	591	8	4	2.3
A3	Skelbro-2	38.7	8.1	591	2	3	2.3
A4	Skelbro-2	15.0	11.2	599	1	7	2.3
A5	Skelbro-2	11.8	7.7	600	4	3	2.3
A6	Skelbro-2	21.1	11.4	602	34	10	2.3

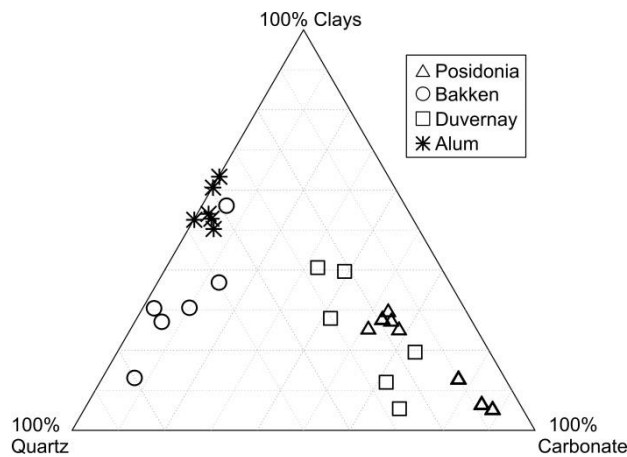
(E) Coal, New Zealand, Cenozoic, Type III

C1*	DEBITS-1	18.9	45.1	414	95	192	0.29
C2*	DEBITS-1	62.5	35.9	414	80	366	0.29
C3*	DEBITS-1	140.5	58.2	419	26	172	0.39
C4*	Rotowaro Mine	Outcrop	61.2	422	32	154	0.45
C5*	Welcome Mine	Outcrop	67.4	424	15	209	0.52

152 *: Samples selected for display in Figures 4 and 5 are covering the whole range of maturity from each location.



153
154 Figure 1: Bulk properties of the sediment pyrolysates concerning alkyl chain length distribution and petroleum
155 type organofacies using the ternary diagram of Horsfield (1989).



156

157 Figure 2: Ternary diagram showing the relative contents of clays, quartz and carbonate minerals for the studied
158 shale samples.

159 **3. Methods**

160 **3.1 Sample extraction**

161 The experimental set up consisted of reaction vessels, equipped with a reflux condenser, in which the
162 samples (10g; previously freeze-dried and ground) were extracted with deionized water (125ml) by
163 heating to 100°C for 48 hours. The water had been treated via UV-photooxidation (Simplicity 185,
164 Millipore) to remove organic compounds prior to the experiments. The extracts were vacuum filtered
165 using 0.45 µm polypropylene filters. The samples were stored at 4°C in the refrigerator and later
166 analyzed by different chromatographic methods. The reproducibility of the extraction was evaluated
167 by running 6 parallel extractions. The standard deviation of the concentration of individual organic
168 acids from the six extracts is below 10% (data not shown).

169 **3.2 Analytical methods**

170 3.2.1 Determination of total organic carbon (TOC) and Rock-Eval Pyrolysis

171 Determination of the total carbon content (TOC) was achieved by measuring the carbon dioxide
172 formed by combustion at 1350°C using a Leco SC-632 IR-detector. Finely crushed rock samples were
173 treated with diluted HCl at 60°C to remove inorganic carbon. The Rock-Eval analyses were performed
174 using a Rock-Eval 6 instrument and following the procedure described in NIGOGA 4th edition (Weiss
175 et al., 2000).

176 3.2.2 Open-system pyrolysis gas chromatography (Py-GC)

177 Open-system Py-GC was applied to all the shale and coal samples. Depending on TOC, up to 35 mg of
178 each crushed sample was placed into a small glass tube, which was sealed and inserted into a Quantum
179 MSSV-2 Thermal Analyzer (Horsfield et al., 1989; Horsfield et al., 2015). The sample was heated in a
180 flow of helium at 300°C for 5 min to get rid of volatile constituents and pollutants. Afterwards, the
181 sample was pyrolyzed at the rate of 50°C min⁻¹ from 300°C to 600°C. Pyrolysis products were

182 collected in a cryogenic trap from which they were later liberated and directly transferred into an
183 Agilent GC 6890A gas chromatograph. Boiling ranges (C_{1-5} , $n-C_{6-14}$ and $n-C_{15+}$) and individual
184 compounds were quantified by external standardization using n -butane.

185 3.2.3 X-ray Diffraction (XRD)

186 The mineral composition of the shale samples was determined by X-ray diffraction (XRD) followed
187 by Rietveld refinement for a quantitative evaluation. XRD analyses were performed using a
188 PANalytical Empyrean. The software EVA (Bruker) was used to identify the minerals and the
189 program AutoQuant for Rietveld calculations was used to determine the amount of the identified
190 minerals (detection limit ~ 1 wt %).

191 3.2.4 Ion chromatography (IC)

192 Extracts were analyzed in replicate by ion chromatography (IC) using conductivity detection (ICS
193 3000, Dionex) to determine the content of organic acids (formate, acetate, propionate, butyrate,
194 valerate and oxalate) and different anions (F^- , PO_4^{3-} , NO_3^- , Cl^- and SO_4^{2-}); the detection limit was about
195 0.1 mg L^{-1} . The equipment used an ASRS Ultra II 2 mm suppressor and a Dionex conductivity detector.
196 For chromatographic separation of the anions the analytical column AS 11 HC (Dionex Corp.) was
197 used at a constant temperature of 35°C . Samples were eluted using KOH solution of varying
198 concentrations over time. The initial KOH concentration was 0.5 mmol L^{-1} and held for 8 min. After
199 10 min, a concentration of 15 mmol L^{-1} KOH was reached and kept constant for 10 min. After 30 min
200 analysis time, a concentration of 60 mmol L^{-1} KOH was reached, followed by a rapid increase to 100
201 mmol L^{-1} reached after 30.2 min analysis time. At 32 min, the KOH concentration was again at the
202 initial level of 0.5 mmol L^{-1} and kept there for an additional 15 min to equilibrate the system. For
203 quantification of organic acids, standards containing all investigated compounds were measured in
204 different concentrations every day. The standard deviation of sample and standard quantification is
205 below 10% (determined by at least two measurements).

206 3.2.5 Liquid chromatography- Dissolved organic carbon (LC-OCD)

207 The characterization and quantification of the dissolved organic carbon (DOC) and its fractions were
 208 conducted by size-exclusion-chromatography (SEC) with subsequent UV ($\lambda=254$ nm) and IR detection
 209 by LC-OCD (Huber and Frimmel, 1996). Phosphate buffer (pH 6.85; $2.7 \text{ g L}^{-1} \text{ KH}_2\text{PO}_4$, 1.6 g L^{-1}
 210 Na_2HPO_4) was used as mobile phase set to a flow of 1.1 mL min^{-1} (Huber et al., 2011). The
 211 chromatographic column was packed with Toyopearl HW-50S resin and had a size of 250×20 mm.
 212 The solid phase separates the components according to their molecular mass, where increasing
 213 retention time indicates decreasing molecular mass (Pelekani et al., 1999). With LC-OCD the organic
 214 matter can be separated into five different fractions referred to as Macro-1 (>10000 Da), Macro-2
 215 (~ 1000 Da), Macro-3 (350-500 Da), Acids (<350 Da) and Neutrals (<350 Da) (Huber et al., 2011)
 216 (Table 2). Constituents of Macro-3 fraction are assumed to reflect breakdown products of constituents
 217 of Macro-2 fraction and are described alternatively as material similar to humic substances but with
 218 lower molecular masses (Huber et al., 2011). The properties and origins of each fraction are shown in
 219 Table 2. The amount of DOC was quantified by IR-detection of released CO_2 after UV-oxidation
 220 ($\lambda=185$ nm) in a Gräntzel thin-film reactor. For molecular mass calibration, humic and fulvic acid
 221 standards of the Suwannee River, provided by the International Humic Substances Society (IHSS),
 222 were used.

223 Table 2 Description of LC-OCD fractions. Modified from Huber et al. (2011) and Penru et al. (2013).

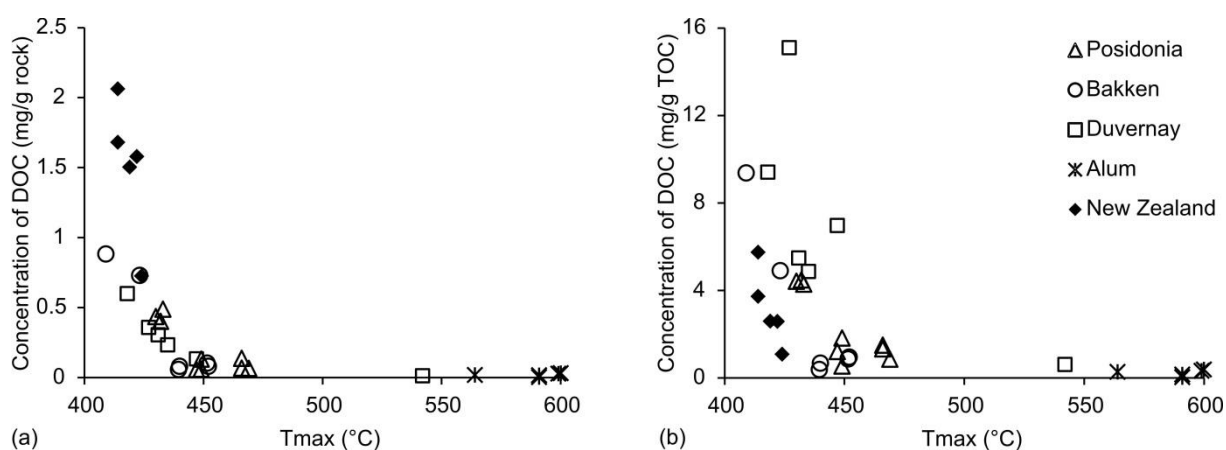
Fraction (This study)	Fraction (Huber et al., 2011)	Molecular mass range	Properties	Description
Macro-1	Biopolymers	>10000 Da	Not UV-absorbable, hydrophilic	Polysaccharides and proteins
Macro-2	Humic substances	~ 1000 Da	Highly UV-absorbable, hydrophobic	Calibration based on Suwannee River standard from IHSS
Macro-3	Building blocks	350-500 Da	UV-absorbable	Breakdown products of humic substances
Acids	Low molecular weight acids	<350 Da	Negatively charged	Low molecular weight aliphatic acids
Neutrals	Low molecular weight neutrals	<350 Da	Weakly or uncharged hydrophilic, amphiphilic	Alcohols, aldehydes, ketones, amino acids

224

225 4. Results

226 4.1 Extraction of DOC

227 The concentrations of DOC versus maturity (T_{max}) for the five series under study are shown in Figure
 228 3. In general, the concentrations of DOC decreased steeply with progressive maturation and then
 229 remained at low values for samples with T_{max} higher than 435°C. The DOC concentrations ranged
 230 from 0.01 to 2.1 mg/g rock (Fig. 3a) or 0.03 to 15.1 mg/g TOC (Fig. 3b), respectively. The amounts of
 231 DOC were comparable in the extracts of Posidonia, Bakken, and Duvernay shales, while the Alum
 232 extracts had the lowest concentrations of DOC and the New Zealand coal extracts showed the highest
 233 DOC concentrations. When the DOC concentration was normalized to TOC of the extracted shales
 234 and coals, the Alum extracts still showed the lowest DOC concentrations but the DOC concentrations
 235 of the New Zealand coal extracts were no longer outstanding (Fig. 3b).



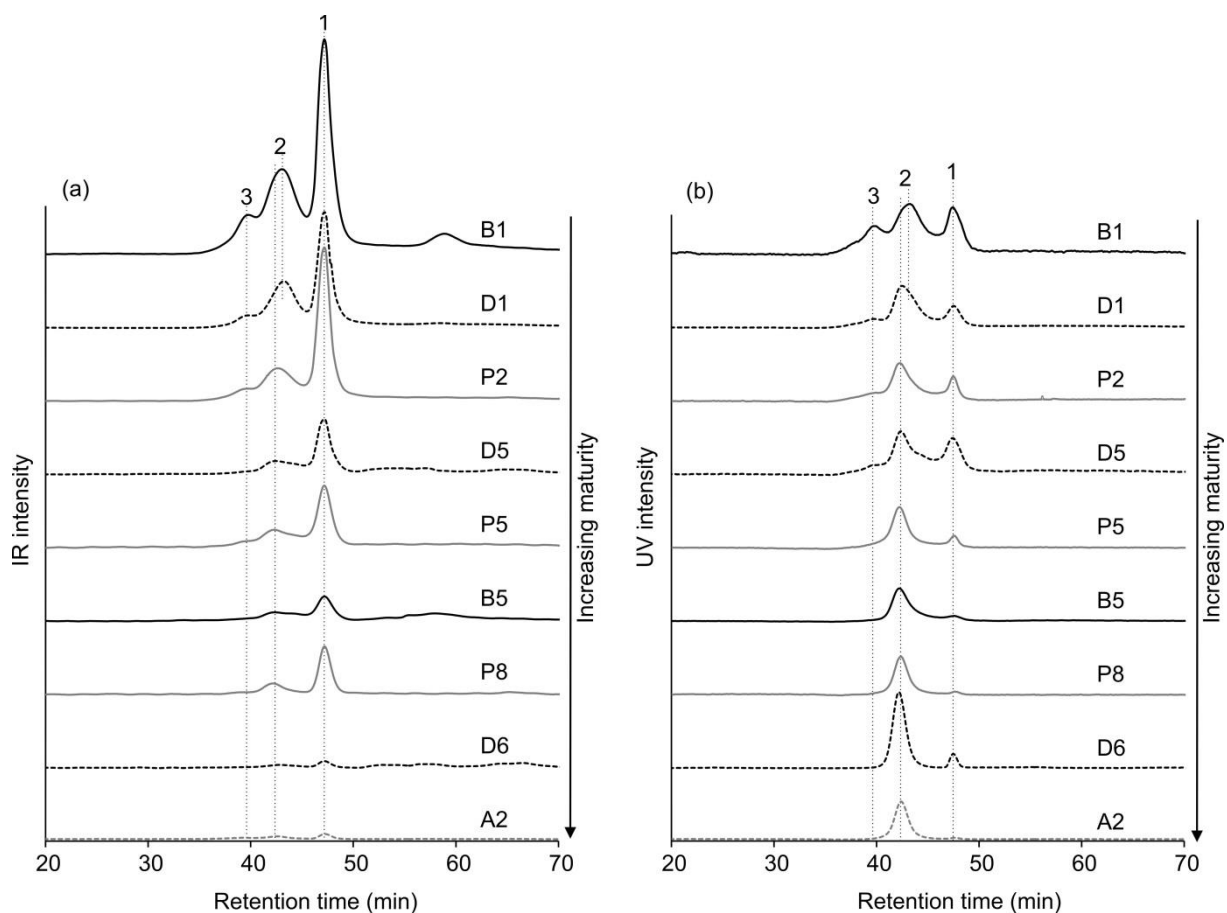
236 (a) 237 Figure 3: DOC concentrations of shale and coal extracts plotted over T_{max} in mg/g rock (a) and in mg/g TOC (b).

238 4.2 Composition of DOC

239 Using size-exclusion chromatography (SEC), DOC can be separated into different fractions according
 240 to their molecular masses. The chromatograms of selected shale extracts are shown in Fig. 4. These
 241 shales have been selected as they represent the whole range of maturity occurring at the different
 242 locations. The DOC of the shale extracts was characterized by one prominent peak (peak 1) at an
 243 elution time of 47.2 min in the IR-chromatogram. This peak was considered to represent the Acid
 244 fraction based on the elution order of authentic standards. Peak 2 was characteristic of the Macro-3
 245 fraction and appeared at a retention time of 42.5 min, except for the extracts of immature samples B1
 246 and D1 where it appeared a little later at 43.1 min. A small peak 3 appearing at 39.8 min represented
 247 the Macro-2 fraction, which is of higher molecular mass than the Macro-3 fraction. The compounds

248 eluting at a later retention time than 50 min correspond to the Neutral fraction. We identified some
249 peaks belonging to the Neutral fraction in both Bakken and Duvernay shale extracts. There is no
250 indication of the Macro-1 fraction in any shale extract.

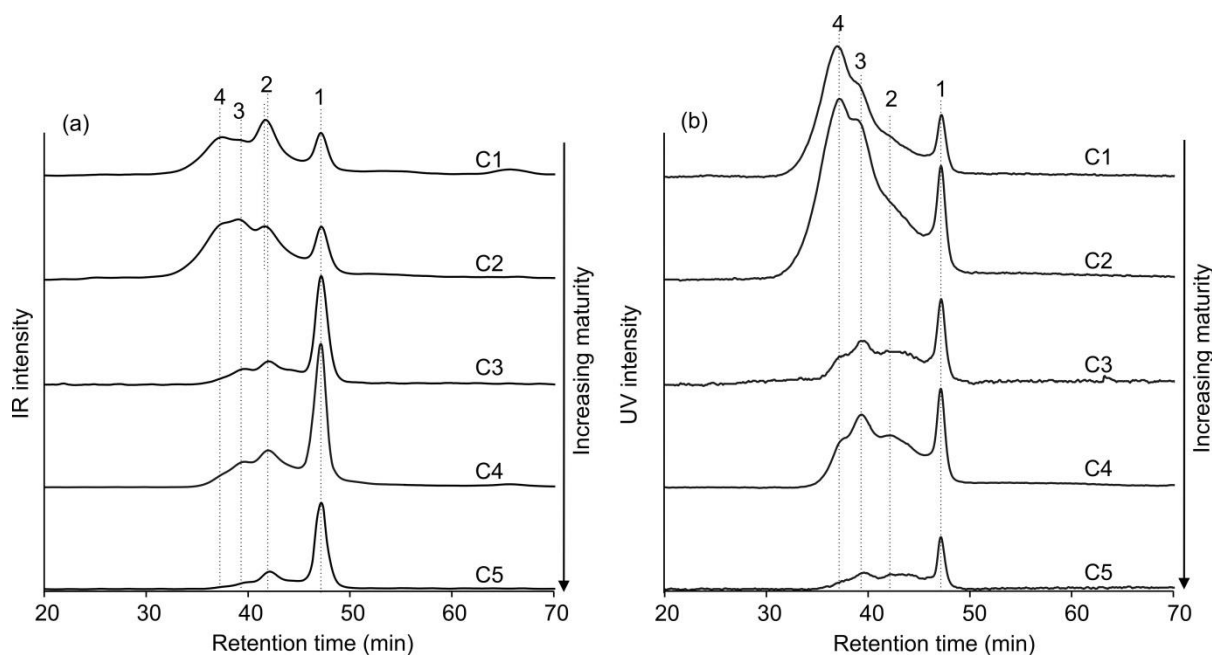
251 Most UV-chromatograms showed two prominent peaks with retention times of 47.2 min (peak 1) and
252 42.5 min (peak 2) except for the extract from B1 that showed a small shift in peak 2 to retention time
253 of 43.1 min. This extract showed an additional peak (peak 3) at retention time of 39.8 min. The peak 3
254 is not observable for the extracts from shales with higher maturity than B1 (Fig. 4b). These parallel
255 peaks indicate the UV-activity of the extracted organic compounds. As the fractions Macro-2 and
256 Macro-3 contain aromatic and unsaturated structures, they have a good UV response (Jacquemet et al.,
257 2005).



258
259 Figure 4: SEC chromatograms giving intensity of (a) IR-signal and (b) UV-signal over run time of the analytical
260 separation of shale extracts.

261 Figure 5a shows the IR-intensities of DOC compositions in coal extracts. Generally, the extracts of
262 coals with $T_{\max} \geq 419^{\circ}\text{C}$ (C3, C4 and C5) showed comparable chromatograms to the shale extracts, but
263 the retention times of the peaks were not exactly identical. Peak 1, indicating the Acid fraction, also
264 eluted after 47.2 min. The peak 2, belonging to the Macro-3 fraction, appeared after 42 min, except for
265 the two lignite extracts of C1 and C2 with retention time of 41.7 min. In general, peak 2 eluted a little
266 earlier than in the shale extracts (42.5min). Peak 3, evaluated as belonging to the Macro-2 fraction,
267 showed a shoulder at retention time of 39 min, which was about 1 min earlier than the peak 3 in the
268 shale extracts. The chromatograms of lignite extracts of C1 and C2 were quite different to the other
269 three extracts from coals of bituminous rank. Here, the Macro-2 was the prominent fraction and an
270 additional peak 4 existed, representing the Macro-2 of higher molecular mass. In general, the extracts
271 show decreasing intensities of the IR-signals with increasing T_{\max} for both shale and coal samples.

272 The corresponding UV-response of the coal extracts is shown in Figure 5b. It is obvious that the UV-
273 chromatograms of shale and coal extracts are quite distinct and the intensity of UV-chromatograms
274 decreases with increasing maturity of the coals. The two lignite extracts of C1 and C2 were
275 comparable with one another in UV-peak distribution and shapes. They both showed a dominant peak
276 at 37 min and a shoulder at 39 min. The two coal extracts of C3 and C4 showed a peak at 39 min and
277 two small shoulders (retention times of 37 and 42 min) on both sides while the coal extract of C5
278 showed the lowest UV-signal. All the coal and shale extracts exhibited a peak at 47.2 minute in the
279 UV-chromatograms, which might correspond to the breakdown products of the Macro-3 fraction or
280 comprise colloidal material where the UV-signal resulted from light scattering rather than absorption
281 (Allpike et al., 2007).

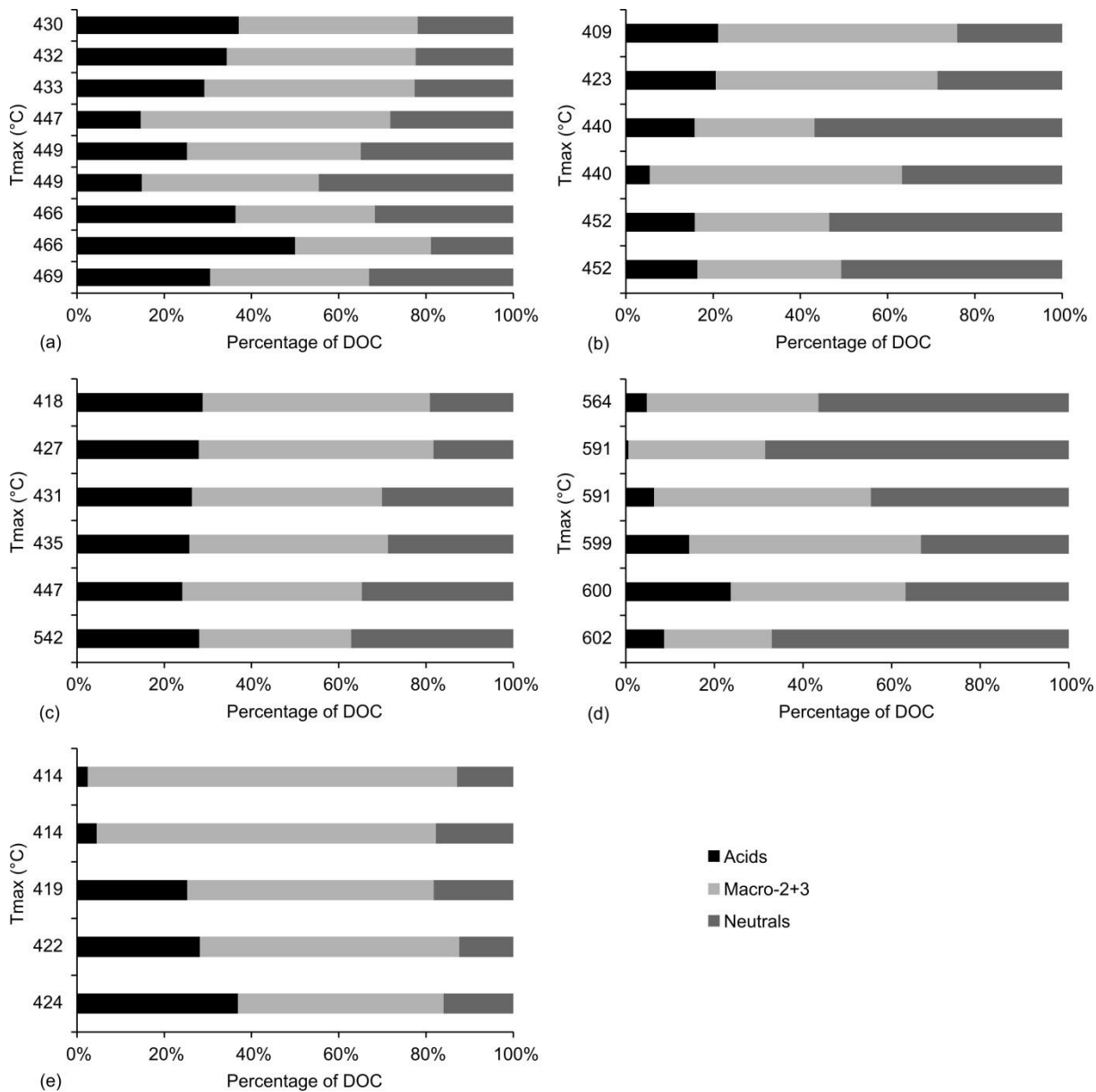


282

283 Figure 5: SEC chromatograms giving intensity of (a) IR-signal and (b) UV-signal over run time of the analytical
 284 separation of coal extracts.

285 The relative percentages of DOC in the different fractions (Acids, Macro-2+3 and Neutrals) are shown
 286 in Figure 6. As the boundary between the fractions Macro-2 and Macro-3 was difficult to identify,
 287 these two fractions were grouped together. For the Posidonia extracts, the percentages of the Acids
 288 decreased with progressive shale maturation up to peak oil window ($T_{\max} = 447^{\circ}\text{C} - 449^{\circ}\text{C}$) and
 289 reversed afterwards. The percentages of the Neutral fraction showed the opposite tendency and the
 290 percentages of the Macro-2+3 fraction showed slight but steady decrease with increasing maturity of
 291 the shales (Fig. 6a). The DOC fractions extracted from the Bakken and Duvernay shales showed
 292 comparable variation (Fig. 6b+c). With increasing maturity of the Bakken and Duvernay shales, the
 293 relative percentages of the Neutral fraction showed a progressive increase, the percentages of the
 294 Macro-2+3 fraction decreased and the Acid fraction decreased only slightly. However, the percentages
 295 of the different fractions were different for Bakken and Duvernay shale extracts. The extracts of the
 296 overmature Alum shales generally showed high percentages of the Neutral fraction and low
 297 percentages of the Acid fraction. As the total amounts of DOC in the leachates of Alum shales were
 298 extremely low, the variations in percentages of different fractions should not be over-interpreted. For
 299 New Zealand coals, the fractions of the two lignite extracts of C1 and C2 showed similar relative

300 distributions of DOC fractions (Neutrals around 15%, Macro-2+3 around 80%, Acids around 5%)
 301 while the percentage of the Acid fraction increased up to 37% and the percentage of the Macro2+3
 302 fractions decreased to 47% for the extracts of the other three bituminous coal samples.



303
 304 Figure 6: The relative percentages of the different DOC fractions extracted from shales and coals, (a) Posidonia
 305 shales; (b) Bakken shales; (c) Duvernay shales; (d) Alum shales; (e) New Zealand coals.

306 4.3 Occurrence of individual organic acids in the extracts

307 4.3.1 The organic acids in shale extracts

308 Formate and acetate were the dominant LMWOAs detected in the water extracts of all shale samples
309 followed by oxalate. Propionate, butyrate and valerate were present in low concentrations in the
310 extracts of immature and some mature samples; none of them were detected in the overmature samples.

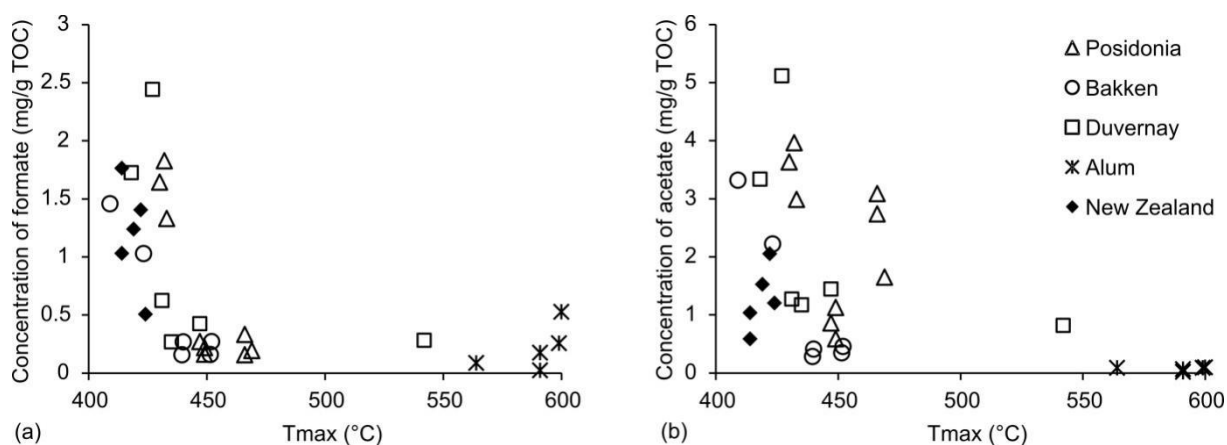
311 The Posidonia shales from the wells Wickensen, Harderode and Haddessen are immature, mature and
312 overmature, respectively (Rullkötter et al., 1988). The concentrations of LMWOAs in the extracts are
313 comparable for samples from the same well, while significant differences can be observed between
314 wells (Fig 7). The concentrations of formate decreased remarkably with increasing maturation of the
315 shales and then remained at a low level for shales reaching the oil window. The concentrations of
316 acetate also decreased with maturity of the shales but surprisingly showed a reversal for shales
317 reaching the gas window – possible explanations for the reversal are discussed later in this paper.

318 The Bakken shale samples were immature to mature and the concentrations of formate and acetate in
319 the extracts were both negatively correlated to thermal maturity, as was the case for the early mature to
320 mature Posidonia samples. No overmature Bakken shale samples were available. The Duvernay shale
321 samples, which were either immature or mature except for one extremely overmature sample, also
322 showed a trend of decreasing carboxylic acid concentrations with increasing maturity. The extracts of
323 the overmature Alum shale had extremely low concentrations of both formate and acetate, which
324 ranged from 0.02 to 0.5 mg/g TOC and 0.02 to 0.10 mg/g TOC, respectively. The reversal in acetate
325 concentration at high maturity as noted for the Posidonia shale extracts was not seen for either the
326 Alum or the Duvernay extracts.

327 4.3.2 Organic acids in coal extracts

328 The concentrations of formate were higher than the concentration of acetate in the extracts of the two
329 lignites while in the extracts of three bituminous coals the concentrations of acetate were higher than
330 formate. Except for oxalate showed much high concentration in the extracts of the two lignites, other
331 acids (e.g. propionate, butyrate, valerate) showed only trace amount or were below the detection limit
332 in all coal extracts. Due to the narrow range of the maturity of the coal samples, the concentration of
333 formate and acetate in the coal extracts was not so obviously correlated with thermal maturity

334 compared to the shale extracts. When normalized to TOC, the concentrations of formate ranged from
 335 0.5 to 1.76 mg/g TOC for coals and from 0.34 to 2.44 mg/g TOC for all shale extracts (Fig. 7a).
 336 The concentrations of formate in the extracts of coals and shales with same maturity were comparable
 337 (Fig. 7a). The concentrations of acetate in the coal extracts were also within the range detected in the
 338 shale extracts, but acetate concentrations were much lower in coal extracts compared to extracts from
 339 shales with the same maturity (Fig. 7b).



340 (a) 341 Figure 7: The concentrations of formate (a) and acetate (b) extracted from shales and coals of different maturities.

342 5. Discussion

343 5.1 Effect of shale and coal organic matter composition on water extracts

344 5.1.1 Bulk DOC and DOC fractions

345 As shown in Fig 3b, only a few permil of the TOC was extracted as DOC in our experiments.
 346 However, the coal samples with higher contents of TOC show higher amount of extracted organic
 347 carbon than the shale samples (Fig. 3a). When normalized to TOC, the concentrations of DOC in the
 348 coal extracts are within the range of the DOC concentrations of the immature shale leachates (Fig. 3b).
 349 From these experimental results, we can conclude that the total amount of extractable organic
 350 compounds from shales and coals was influenced by the amount of TOC and probably not by the
 351 kerogen type of the organic matter. Nevertheless, the DOC compositions of shale and coal extracts are
 352 clearly influenced by the kerogen types, as shown by the differences in IR-chromatograms of the
 353 extracts. The two lignite extracts of C1 and C2 are characterized in their IR-chromatograms by high
 354 intensities of the Macro-2+3 fractions while the IR-chromatograms of the other three coal extracts (C3,

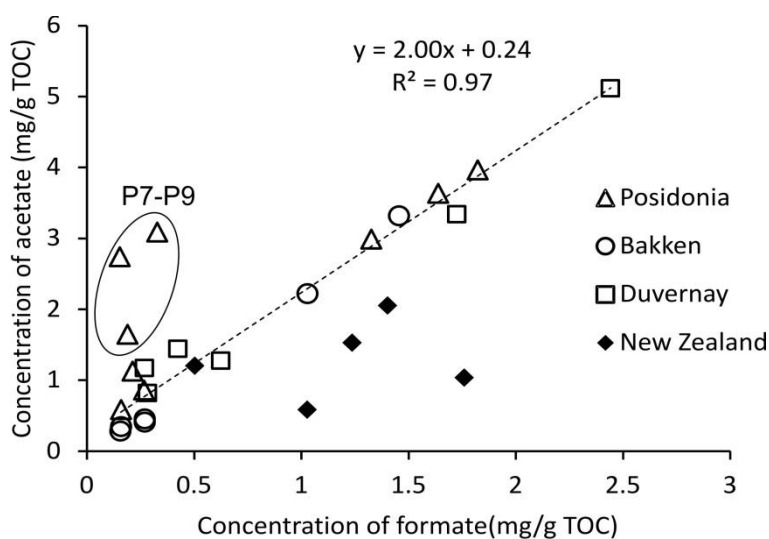
355 C4 and C5) show high peaks of the Acid fraction, which are similar to the chromatographic patterns of
356 the immature shale extracts. The organic matter of coals C4 and C5 contains mainly terrestrial higher
357 plant material with a significant contribution of microbial biomass (Vu et al., 2009) and it can be as
358 *previous* sumed that the organic matter of C3 also has a significant contribution of microbial biomass
359 as it belongs to a similar petroleum type organofacies as coals C4 and C5 (Fig. 1). Also all selected
360 shales have organic matter that is derived from a mixture of planktonic and microbial sources.
361 Therefore, the similarity of the chromatographic patterns is plausible. However, the retention times of
362 the peak maxima of the Macro-2 and Macro-3 fractions from the coal extracts are shorter than for the
363 shale extracts, which points to the differences in the molecular masses of these DOC fractions from
364 shales and coals. The molecular masses of most constituents included in the fractions Macro-2 and
365 Macro-3 in the coal extracts are heavier than in shale extracts. Even more notable differences between
366 shale and coal extracts can be observed in the UV-chromatograms where coal extracts showed higher
367 intensities. These higher intensities may be related to the presence of aromatic structures in the DOC
368 of coal extracts. Coals with type III kerogen mainly originate from terrigenous higher plant material of
369 lignocellulosic origin while the shales with type II kerogen originate from marine planktonic material
370 which is comprised of aliphatic structures.

371 5.1.2 LMWOAs

372 The observed distribution of the individual organic acid concentrations, where acetate is dominant in
373 the shale and bituminous coal extracts, is in accordance with the results from hydrous pyrolysis of
374 kerogen (Kawamura et al., 1986), crude oils (Borgund and Barth, 1994) and source rocks (Barth and
375 Bjørlykke, 1993; Barth et al., 1988). The observed order in concentrations with acetate >> propionate >
376 butyrate > valerate has also been reported for natural deep subsurface waters (Fisher, 1987; Means and
377 Hubbard, 1987). However, no information about formate concentrations was given in these previous
378 studies.

379 The relation between the concentrations of formate and acetate, extracted from shales and coals is
380 shown in Figure 8. The results of Alum shale extracts are not included here due to their extremely low
381 concentrations. A linear correlation between the concentrations of formate and acetate can be observed

382 in all shale extracts except for the three Posidonia extracts of P7, P8 and P9 and the coal extracts. This
 383 linear trend indicates that the extraction of these acids might be controlled by the same factors.
 384 Discussion about the three outlier points representing the three Posidonia extracts of P7, P8 and P9 is
 385 given later in this paper. The linear correlation between the concentrations of formate and acetate in
 386 the shale extracts cannot be observed in the coal extracts. This may be due to the fact that the five
 387 samples already represent two different petroleum type organofacies. Thus, we can deduce that the
 388 correlation between the concentrations of formate and acetate in the extracts of samples with the same
 389 organofacies might be similar.



390
 391 Figure 8: Comparison of formate and acetate concentrations in the water extracts. The linear regression excludes
 392 the extracts of P7, P8 and P9 and New Zealand coals.

393 5.2 Effect of burial processes on composition of water extracts

394 5.2.1 Influence of maturation on the extracted organic matter

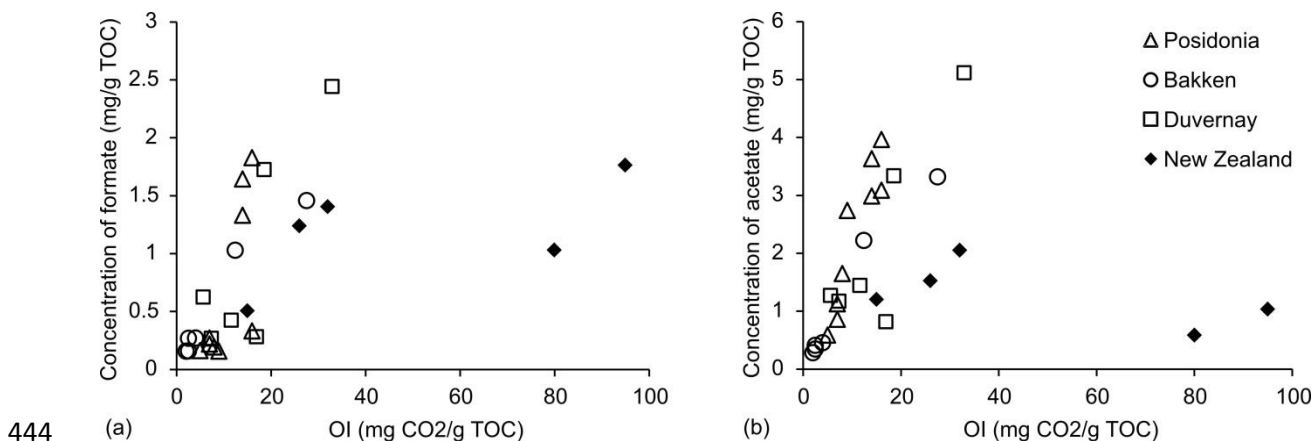
395 As illustrated in Fig. 3, the concentrations of DOC decreased with maturity until T_{max} reaches 435°C
 396 after which low concentrations were maintained. The samples clearly showed a higher potential for
 397 DOC extraction at the stage of diagenesis rather than at later stages when thermal cracking reactions
 398 became significant. Generally, the concentrations of the individual DOC fractions also decreased with
 399 increasing maturity for shale samples from the same formation, which could be indicated by the IR-
 400 chromatograms as the intensities of the IR-chromatograms correspond to the concentrations of DOC

401 (Fig. 4a). But there was no overall trend of decreasing DOC concentration with increasing maturity.
402 This can be illustrated for shale D1 which is less mature (lower T_{\max}) than shale P2 but the extract of
403 D1 had a lower DOC concentration (lower IR signal intensity). The similar phenomenon can also be
404 observed for samples B5 and P8. Though the coal samples represent only a very narrow range in
405 maturity, the general trend of decreasing DOC concentrations with increasing T_{\max} can also be
406 observed for the coal extracts.

407 Fig. 7 showed the concentrations of formate and acetate in extracts over T_{\max} of the shales/coal. The
408 concentrations of extracted acids decreased with increasing maturity of the samples except for the
409 overmature Posidonia shales from the Haddessen well. Here, acetate concentrations are higher than
410 expected. This similar decreasing tendency of LMWOA concentrations in extracts with ongoing
411 maturation has already been described in the experiments of soxhlet water extraction and alkaline ester
412 cleavage of coals (Glombitza et al., 2009; Vieth et al., 2008). Thus, it may be assumed that a potential
413 equilibrium exists between kerogen bound LMWOAs and free LMWOAs. Kerogen is generally
414 accepted as the source of LMWOAs and their generation is considered to result from kerogen
415 maturation (Eglinton et al., 1987; Kawamura and Kaplan, 1987). The immature kerogen maturation
416 process simulated by hydrous pyrolysis illustrates that the generation of LMWOAs from kerogen
417 resulted from cracking and hydrolysis reactions and continues at high simulated maturation levels
418 (Barth et al., 1988; Kawamura et al., 1986). In the present experiment, the LMWOAs easily extracted
419 during water extraction were assumed to be mainly the free acids, which assimilated into sedimentary
420 organic matter or dissolved in the in-situ pore water during early diagenesis (Pittman and Lewan,
421 1994). The immature kerogen contains significant amounts of aliphatic components and oxygen. Their
422 functional groups show higher potential to form LMWOAs compared to the overmature kerogen,
423 which contains fewer aliphatic chains and less oxygen (Bernard et al., 2012; Vu et al., 2013). The
424 defunctionalisation reaction of oxygen containing functional groups and oxidation of *n*-alkanes during
425 geological times might lead to the formation of LMWOAs. So the maturity of the samples is a pivotal
426 factor that influences the concentrations of different acids in the extracts. This is supported by the
427 minor amounts of formate and acetate extracted from overmature Alum shale samples.

428 5.2.2 Influence of OI on the concentration of individual organic acids

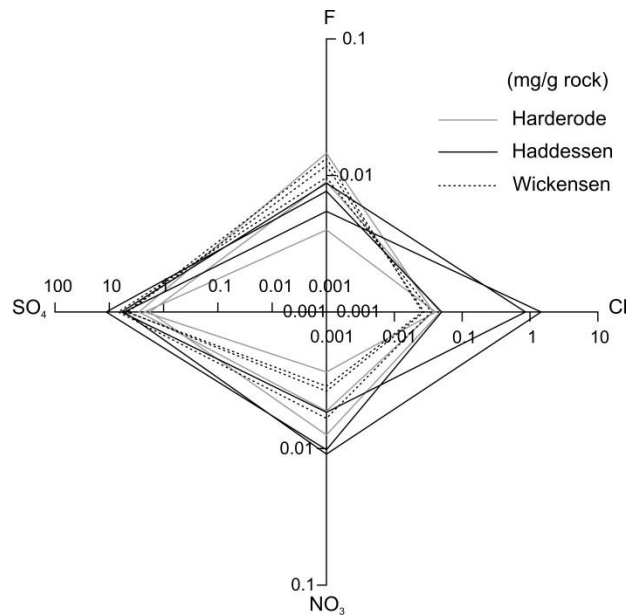
429 The significant decrease of oxygen-containing compounds during diagenesis can be traced using van
430 Krevelen diagram, which shows the preferential decrease of O/C ratio relative to H/C ratio (Tissot and
431 Welte, 1984). Furthermore, the loss of C=O functionalities with increasing maturity can be revealed
432 by infrared spectroscopy (al Sandouk-Lincke et al., 2013; Lis et al., 2005). A general positive
433 correlation between Oxygen Index (OI) and the concentrations of formate and acetate in the extracts
434 could be observed for the Bakken, Posidonia and Duvernay (Fig. 9). This indicates that the amounts of
435 acids extracted from the shales were directly constrained by the initial kerogen oxygen content. When
436 the coals were separated into two groups according to their organofacies, the positive trend between
437 OI of coals and the concentrations of formate and acetate in the extracts also could be observed in each
438 group. The coal samples with type III kerogen, characterized by generally high atomic O/C ratio, were
439 expected to generate a higher concentration of organic acids than type II kerogen (Cooles et al., 1987).
440 But the functionality of the oxygen may be an important factor, i.e. oxygen in carboxylic acids and
441 esters is assumed to contribute more to LMWOAs than the oxygen in ether bonds and ring systems
442 (Borgund and Barth, 1994). Additionally, the type II kerogen contains more aliphatic moieties that can
443 be oxidized to form carboxylic acids.



445 Figure 9: Concentrations of formate (a) and acetate (b) in the extracts are plotted over the oxygen index (OI)
446 values of the shales and coals.

447 5.2.3 Possible influence of hydrothermal brines

448 The unexpectedly high concentrations of acetate extracted from these overmature Posidonia shales
449 might be related to the occurrence of hydrothermal fluid migration along the southern rim of the
450 Lower Saxony Basin (Petmecky et al., 1999). The occurrence of authigenic albite with halite
451 inclusions has been used to argue for hydrothermal activity affecting the mineralogy of the Posidonia
452 shale (Bernard et al., 2012). The hydrothermal brines and iron-bearing minerals may have provided a
453 source of available oxygen to partly oxidize bitumen to form acids (Bernard et al., 2012). The
454 oxidation of hydrocarbons may produce LMWOAs during thermal maturation (Barth, 1987; Borgund
455 and Barth, 1994; Eglinton et al., 1987; Seewald, 2001b; Surdam et al., 1993), and this is speculated to
456 be the main control on the high concentration of acetate in the extracts of samples P7, P8 and P9. The
457 higher concentrations of chloride detected in the extracts of shales from the overmature Haddessen
458 well in comparison to the extracts of other Posidonia shales would support an influence of
459 hydrothermal brines (Fig. 10). Hydrothermal activity could have provided both a local heat source to
460 drive the generation reactions which led to the formation of organic acids, and water to act as reaction
461 and transport medium. It should be noted that high geothermal gradients associated with hydrothermal
462 activity might have also increased the rate of acid production from kerogen. The steep gradient in
463 formate/acetate for the Haddessen shales (P7-P9; Fig. 8) might signal the selective generation of
464 acetate from bitumen precursors, possibly accompanied by formate degradation or consumption.
465 Though a heat-flow anomaly existed in the Bakken formation (Kuhn et al., 2012), no obvious
466 influence on the generation of acetate or formate could be observed in our experiments.



467

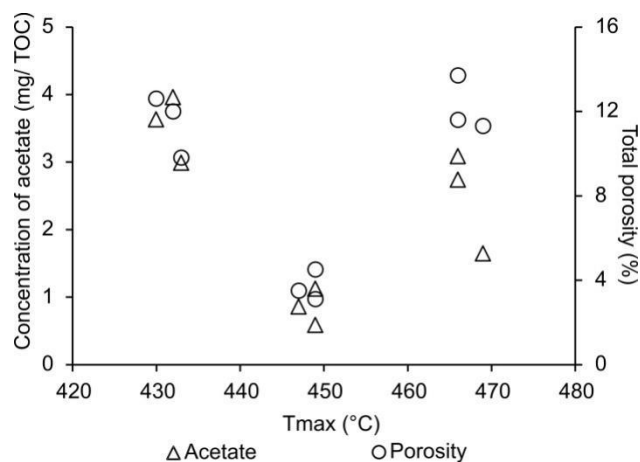
468

469 Figure 10: The concentrations of inorganic anions in Posidonia extracts. The concentrations of fluoride, sulfate
 470 and nitrate are in the same order of magnitude for most Posidonia samples, only extracts of P8 and P9 show
 471 extremely high concentrations of chloride.

472 5.2.4 Correlation between concentration of acids and porosity

473 LMWOAs have been shown to be an important potential contributor to generate secondary porosity by
 474 dissolution of aluminosilicate and carbonate minerals (Surdam et al., 1984). That type of porosity
 475 could provide more space for storage of generated bitumen in shales, which could then act as a source
 476 of acetate afterwards. The total porosity of the Posidonia maturity sequence shows a loss of porosity in
 477 going from the immature stage (ca. 10-13%) to the oil window (4-6%) and then an increase again in
 478 the gas window Haddessen well (9-12%) (Mathia et al., 2013). The pattern in porosity changes with
 479 increasing maturity correlates with the concentration of acetate in the water extracts of the respective
 480 shales (Fig. 11), but not with formate. According to Bernard et al. (2012), the pores in Posidonia
 481 shales of oil window maturity were filled by viscous bitumen during kerogen degradation, and this
 482 resulted in the decrease of porosity. In gas window, the porosity increased again because of secondary
 483 cracking reactions leading to the generation and exsolution of gaseous hydrocarbons. The creation of
 484 nanoporosity within overmature Barnett shale by thermal cracking of retained hydrocarbons has also

485 been reported by Loucks et al. (2009). Based on the lack of porosity data from other shales, no reliable
486 evaluation of the correlation between extracted acetate concentrations and porosity of Posidonia shales
487 is possible. It is assumed that there is no cause-effect relationship between these parameters.



488
489 Figure 11: The variation of acetate concentrations in Posidonia extracts (left Y axis) and porosities of the shales
490 (right Y axis) with increasing maturity.

491 6. Summary and Conclusions

492 Extraction of black shales and coals using deionized water resulted in the release of water soluble
493 organic compounds. In general, the concentrations of DOC decreased steeply with progressive
494 maturation and then remained at low values for samples with T_{max} higher than 435°C. The coal
495 extracts showed much higher DOC concentrations on a per gram sediment basis, but when normalized
496 to TOC, the concentrations of DOC are within the range observed for the immature shale leachates.
497 From this we conclude that maturity of the kerogen and TOC content are two main factors that
498 influence the amount of DOC extracted from sediments. Macro-2, Macro-3, Acids and Neutrals
499 comprise the four DOC fractions that have been detected in the extracts using SEC. The extracts of
500 immature samples have a high content of the Macro-2 and Macro-3 fractions whereas leachates of
501 mature and overmature samples are dominated by the Neutral fraction, which represent the final
502 degradation products of organic matter during geological maturation. The DOC extracted from coal
503 samples is more aromatic than that extracted from shales, which is documented by the higher intensity
504 of UV-signals. According to the retention times in SEC, it can be deduced that the molecular weight of

505 the constituents included in the fractions Macro-2 and Macro-3 of the coal extracts is higher than for
506 the shale extracts.

507 Acetate and formate represent the dominant acids extracted from shales and coals. Other LMW mono-
508 and di-carboxylic acids like propionate and oxalate are detected in some of the leachates, but in lower
509 concentrations. The linear trend between the concentrations of formate and acetate extracted from
510 shales indicated that the generation of individual LMWOAs is controlled by the same factor. The
511 concentrations of acids also decreased with increasing maturity of the shales except for the overmature
512 Posidonia shales from the Haddessen well. The reason for the high concentrations of acetate in the
513 extracts of overmature Haddessen shales might be the influence of hydrothermal brines. These brines
514 might provide oxygen and hydrogen to enhance the generation of organic acids.

515 **Acknowledgments**

516 The financial support from the China Scholarship Council (CSC) for Yaling Zhu is gratefully
517 acknowledged. The authors thank Kristin Günther and Wilma Mierke (GFZ Potsdam) for their
518 excellent technical assistance in the lab. We appreciate the North Dakota Geological Survey and the
519 Canadian Geological Survey for providing samples. The two anonymous reviewers are greatly
520 acknowledged for their useful comments.

521 **References**

- 522 al Sandouk-Lincke, N.A., Schwarzbauer, J., Volk, H., Hartkopf-Fröder, C., Fuentes, D., Young, M., Littke,
523 R., 2013. Alteration of organic material during maturation: A pyrolytic and infrared spectroscopic
524 study of isolated bisaccate pollen and total organic matter (Lower Jurassic, Hils Syncline, Germany).
525 *Organic Geochemistry* 59, 22-36.
- 526 Allpike, B.P., Heitz, A., Joll, C.A., Kagi, R.I., 2007. A new organic carbon detector for size exclusion
527 chromatography. *Journal of Chromatography A* 1157, 472-476.
- 528 Barth, T., 1987. Multivariate analysis of aqueous organic acid concentrations and geological
529 properties of north sea reservoirs. *Chemometrics and Intelligent Laboratory Systems* 2, 155-160.
- 530 Barth, T., Bjørlykke, K., 1993. Organic acids from source rock maturation: generation potentials,
531 transport mechanisms and relevance for mineral diagenesis. *Applied Geochemistry* 8, 325-337.
- 532 Barth, T., Borgund, A.E., Hopland, A.L., Graue, A., 1988. Volatile organic acids produced during
533 kerogen maturation— amounts, composition and role in migration of oil. *Organic Geochemistry* 13,
534 461-465.
- 535 Bernard, S., Horsfield, B., Schulz, H.-M., Schreiber, A., Wirth, R., Anh Vu, T.T., Perssen, F., Könitzer, S.,
536 Volk, H., Sherwood, N., Fuentes, D., 2010. Multi-scale detection of organic and inorganic signatures

537 provides insights into gas shale properties and evolution. *Chemie der Erde - Geochemistry* 70,
538 Supplement 3, 119-133.

539 Bernard, S., Horsfield, B., Schulz, H.-M., Wirth, R., Schreiber, A., Sherwood, N., 2012. Geochemical
540 evolution of organic-rich shales with increasing maturity: A STXM and TEM study of the Posidonia
541 Shale (Lower Toarcian, northern Germany). *Marine and Petroleum Geology* 31, 70-89.

542 Borgund, A.E., Barth, T., 1994. Generation of short-chain organic acids from crude oil by hydrous
543 pyrolysis. *Organic Geochemistry* 21, 943-952.

544 Bou-Raad, M., Hobday, M.D., Rix, C.J., 2000. Aqueous extraction of oxalate and other anions from
545 coal. *Fuel* 79, 1185-1193.

546 Bu, X., Wang, L., Ma, W., Yu, X., McDowell, W.H., Ruan, H., 2010. Spectroscopic characterization of
547 hot-water extractable organic matter from soils under four different vegetation types along an
548 elevation gradient in the Wuyi Mountains. *Geoderma* 159, 139-146.

549 Buchardt, B., Clausen, J., Thomsen, E., 1986. Carbon isotope composition of lower palaeozoic
550 kerogen: Effects of maturation. *Organic Geochemistry* 10, 127-134.

551 Buchardt, B., Lewan, M.D., 1990. Reflectance of vitrinite-like macerals as a thermal maturity index for
552 Cambrian-Ordovician Alum Shale, southern Scandinavia. *AAPG Bulletin* 74, 394-406.

553 Chow, N., Wendte, J., Stasiuk, L.D., 1995. Productivity versus preservation controls on two organic-
554 rich carbonate facies in the Devonian of Alberta; sedimentological and organic petrological evidence.
555 *Bulletin of Canadian Petroleum Geology* 43, 433-460.

556 Cooles, G.P., Mackenzie, A.S., Parkes, R.J., 1987. Non-hydrocarbons of significance in petroleum
557 exploration: volatile fatty acids and nonhydrocarbon gases. *Mineralogical Magazine* 51, 483-493.

558 Creaney, S., Allan, J., 1990. Hydrocarbon generation and migration in the Western Canada
559 sedimentary basin. Geological Society, London, Special Publications 50, 189-202.

560 Dembicki, H., Pirkle, F.L., 1985. Regional source rock mapping using a source potential rating index.
561 *AAPG Bulletin* 69, 567-581.

562 Dieckmann, V., 1999. The prediction of the oil and gas composition by the integration of laboratory
563 experiments and case studies. RWTH Aachen University, PhD Thesis, p. 285. ISSN 0944-2952.

564 Dieckmann, V., Fowler, M., Horsfield, B., 2004. Predicting the composition of natural gas generated
565 by the Duvernay Formation (Western Canada Sedimentary Basin) using a compositional kinetic
566 approach. *Organic Geochemistry* 35, 845-862.

567 Dobson, K.R., Stephenson, M., Greenfield, P.F., Bell, P.R.F., 1985. Identification and treatability of
568 organics in oil shale retort water. *Water research* 19, 849-856.

569 Eglinton, T.I., Curtis, C.D., Rowland, S.J., 1987. Generation of water-soluble organic acids from
570 kerogen during hydrous pyrolysis: implications for porosity development. *Mineralogical Magazine* 51,
571 495-503.

572 Fisher, J.B., 1987. Distribution and occurrence of aliphatic acid anions in deep subsurface waters.
573 *Geochimica et Cosmochimica Acta* 51, 2459-2468.

574 Ghani, A., Dexter, M., Perrott, K.W., 2003. Hot-water extractable carbon in soils: a sensitive
575 measurement for determining impacts of fertilisation, grazing and cultivation. *Soil Biology and*
576 *Biochemistry* 35, 1231-1243.

577 Glombitza, C., 2011. *New Zealand Coals - a Potential Feedstock for Deep Microbial Life.*
578 Omniscryptum GmbH & Company KG.

579 Glombitza, C., Mangelsdorf, K., Horsfield, B., 2009. A novel procedure to detect low molecular weight
580 compounds released by alkaline ester cleavage from low maturity coals to assess its feedstock
581 potential for deep microbial life. *Organic Geochemistry* 40, 175-183.

582 Gregorich, E.G., Beare, M.H., Stoklas, U., St-Georges, P., 2003. Biodegradability of soluble organic
583 matter in maize-cropped soils. *Geoderma* 113, 237-252.

584 Herbert, B.E., Bertsch, P.M., 1995. Characterization of dissolved and colloidal organic matter in soil
585 solution: A review. In *Carbon forms and functions in forest soils.* J. M. Kelly and W. W. McFee (eds.).
586 SSSA, Madison, WI, 63-88.

587 Horsfield, B., 1989. Practical criteria for classifying kerogens: Some observations from pyrolysis-gas
588 chromatography. *Geochimica et Cosmochimica Acta* 53, 891-901.

589 Horsfield, B., Disko, U., Leistner, F., 1989. The micro-scale simulation of maturation: outline of a new
590 technique and its potential applications. *Geol Rundsch* 78, 361-373.

591 Horsfield, B., Leistner, F., Hall, K., 2015. CHAPTER 7 Microscale Sealed Vessel Pyrolysis, Principles and
592 Practice of Analytical Techniques in Geosciences. The Royal Society of Chemistry, pp. 209-250.

593 Horsfield, B., Schenk, H.J., Mills, N., Welte, D.H., 1992. An investigation of the in-reservoir conversion
594 of oil to gas: compositional and kinetic findings from closed-system programmed-temperature
595 pyrolysis. *Organic Geochemistry* 19, 191-204.

596 Horsfield, B., Schenk, H.J., Zink, K., Ondrak, R., Dieckmann, V., Kallmeyer, J., Mangelsdorf, K., di
597 Primio, R., Wilkes, H., Parkes, R.J., Fry, J., Cragg, B., 2006. Living microbial ecosystems within the
598 active zone of catagenesis: Implications for feeding the deep biosphere. *Earth and Planetary Science
599 Letters* 246, 55-69.

600 Huber, S.A., Balz, A., Abert, M., Pronk, W., 2011. Characterisation of aquatic humic and non-humic
601 matter with size-exclusion chromatography – organic carbon detection – organic nitrogen detection
602 (LC-OCD-OND). *Water research* 45, 879-885.

603 Huber, S.A., Frimmel, F.H., 1996. Size-exclusion-chromatography with organic carbon detection (LC-
604 OCD): A fast and reliable method for the characterization of hydrophilic organic matter in natural
605 waters. *Vom Wasser* 86, 277–290.

606 Jacquemet, V., Gaval, G., Rosenberger, S., Lesjean, B., Schrotter, J.C., 2005. Towards a better
607 characterisation and understanding of membrane fouling in water treatment. *Desalination* 178, 13-
608 20.

609 Jarvie, D.M., Hill, R.J., Ruble, T.E., Pollastro, R.M., 2007. Unconventional shale-gas systems: The
610 Mississippian Barnett Shale of north-central Texas as one model for thermogenic shale-gas
611 assessment. *AAPG Bulletin* 91, 475-499.

612 Jiang, C., Li, M., 2002. Bakken/Madison petroleum systems in the Canadian Williston Basin. Part 3:
613 geochemical evidence for significant Bakken-derived oils in Madison Group reservoirs. *Organic
614 Geochemistry* 33, 761-787.

615 Jiang, C., Li, M., Osadetz, K.G., Snowdon, L.R., Obermajer, M., Fowler, M.G., 2001. Bakken/Madison
616 petroleum systems in the Canadian Williston Basin. Part 2: molecular markers diagnostic of Bakken
617 and Lodgepole source rocks. *Organic Geochemistry* 32, 1037-1054.

618 Kallmeyer, J., Mangelsdorf, K., Cragg, B., Horsfield, B., 2006. Techniques for Contamination
619 Assessment During Drilling for Terrestrial Subsurface Sediments. *Geomicrobiology Journal* 23, 227-
620 239.

621 Kawamura, K., Kaplan, I.R., 1987. Dicarboxylic acids generated by thermal alteration of kerogen and
622 humic acids. *Geochimica et Cosmochimica Acta* 51, 3201-3207.

623 Kawamura, K., Tannenbaum, E., Huizinga, B.J., Kaplan, I.R., 1986. Volatile organic acids generated
624 from kerogen during laboratory heating. *Geochem J* 20, 51-59.

625 Kelemen, S.R., Afeworki, M., Gorbaty, M.L., Sansone, M., Kwiatek, P.J., Walters, C.C., Freund, H.,
626 Siskin, M., Bence, A.E., Curry, D.J., Solum, M., Pugmire, R.J., Vandenbroucke, M., Leblond, M., Behar,
627 F., 2007. Direct Characterization of Kerogen by X-ray and Solid-State ¹³C Nuclear Magnetic
628 Resonance Methods. *Energy & Fuels* 21, 1548-1561.

629 Kharaka, Y.K., Carothers, W.W., Rosenbauer, R.J., 1983. Thermal decarboxylation of acetic acid:
630 Implications for origin of natural gas. *Geochimica et Cosmochimica Acta* 47, 397-402.

631 Kuhn, P., Primio, R.D., Horsfield, B., 2010. Bulk composition and phase behaviour of petroleum
632 sourced by the Bakken Formation of the Williston Basin. Geological Society, London, Petroleum
633 Geology Conference 7, 1065-1077.

634 Kuhn, P.P., di Primio, R., Hill, R., Lawrence, J.R., Horsfield, B., 2012. Three-dimensional modeling
635 study of the low-permeability petroleum system of the Bakken Formation. *Aapg Bulletin* 96, 1867-
636 1897.

637 Leenheer, J.A., Croué, J.-P., 2003. Peer Reviewed: Characterizing Aquatic Dissolved Organic Matter.
638 *Environmental Science & Technology* 37, 18A-26A.

639 Leenheer, J.A., Noyes, T.I., Stuber, H.A., 1982. Determination of polar organic solutes in oil-shale
640 retort water. *Environmental Science & Technology* 16, 714-723.

641 Leenheer, M.J., 1984. Mississippian Bakken and equivalent formations as source rocks in the Western
642 Canadian Basin. *Organic Geochemistry* 6, 521-532.

643 Lepane, V., Leeben, A., Malashenko, O., 2004. Characterization of sediment pore-water dissolved
644 organic matter of lakes by high-performance size exclusion chromatography. *Aquat. Sci.* 66, 185-194.

645 Lester, Y., Ferrer, I., Thurman, E.M., Sitterley, K.A., Korak, J.A., Aiken, G., Linden, K.G., 2015.
646 Characterization of hydraulic fracturing flowback water in Colorado: Implications for water treatment.
647 *Science of The Total Environment* 512–513, 637-644.

648 Li, M., Yao, H., Stasiuk, L.D., Fowler, M.G., Larter, S.R., 1997. Effect of maturity and petroleum
649 expulsion on pyrrolic nitrogen compound yields and distributions in Duvernay Formation petroleum
650 source rocks in central Alberta, Canada. *Organic Geochemistry* 26, 731-744.

651 Lis, G.P., Mastalerz, M., Schimmelmann, A., Lewan, M.D., Stankiewicz, B.A., 2005. FTIR absorption
652 indices for thermal maturity in comparison with vitrinite reflectance R₀ in type-II kerogens from
653 Devonian black shales. *Organic Geochemistry* 36, 1533-1552.

654 Littke, R., Baker, D.R., Leythaeuser, D., 1988. Microscopic and sedimentologic evidence for the
655 generation and migration of hydrocarbons in Toarcian source rocks of different maturities. *Organic*
656 *Geochemistry* 13, 549-559.

657 Littke, R., Leythaeuser, D., Rullkötter, J., Baker, D.R., 1991. Keys to the depositional history of the
658 Posidonia Shale (Toarcian) in the Hils Syncline, northern Germany. *Geological Society, London,*
659 *Special Publications* 58, 311-333.

660 Loucks, R.G., Reed, R.M., Ruppel, S.C., Jarvie, D.M., 2009. Morphology, Genesis, and Distribution of
661 Nanometer-Scale Pores in Siliceous Mudstones of the Mississippian Barnett Shale. *J Sed Res* 79, 848-
662 861.

663 Maguire-Boyle, S.J., Barron, A.R., 2014. Organic compounds in produced waters from shale gas wells.
664 *Environmental Science-Processes & Impacts* 16, 2237-2248.

665 Mann, U., Müller, P.J., 1988. Source rock evaluation by well log analysis (Lower Toarcian, Hils
666 syncline). *Organic Geochemistry* 13, 109-119.

667 Mathia, E., Rexer, T., Bowen, L., Aplin, A., 2013. Evolution of porosity and pore systems in organic-
668 rich Posidonia and Wealden Shales, 75th EAGE Conference & Exhibition incorporating SPE EUROPEC
669 2013. ISBN 2214-4609.

670 Means, J.L., Hubbard, N., 1987. Short-chain aliphatic acid anions in deep subsurface brines: A review
671 of their origin, occurrence, properties, and importance and new data on their distribution and
672 geochemical implications in the Palo Duro Basin, Texas. *Organic Geochemistry* 11, 177-191.

673 Muscio, G.P.A., Horsfield, B., Welte, D.H., 1994. Occurrence of thermogenic gas in the immature
674 zone—implications from the Bakken in-source reservoir system. *Organic Geochemistry* 22, 461-476.

675 Olsson, O., Weichgrebe, D., Rosenwinkel, K.-H., 2013. Hydraulic fracturing wastewater in Germany:
676 composition, treatment, concerns. *Environmental earth sciences* 70, 3895-3906.

677 Orem, W., Tatu, C., Varonka, M., Lerch, H., Bates, A., Engle, M., Crosby, L., McIntosh, J., 2014. Organic
678 substances in produced and formation water from unconventional natural gas extraction in coal and
679 shale. *International Journal of Coal Geology* 126, 20-31.

680 Pelekani, C., Newcombe, G., Snoeyink, V.L., Hepplewhite, C., Assemi, S., Beckett, R., 1999.
681 Characterization of Natural Organic Matter Using High Performance Size Exclusion Chromatography.
682 *Environmental Science & Technology* 33, 2807-2813.

683 Penru, Y., Simon, F.X., Guastalli, A., Esplugas, S., Llorens, J., 2013. Characterization of natural organic
684 matter from Mediterranean coastal seawater. *Aqua* 62, 42-51.

685 Petersen, H.I., Rosenberg, P., Nytoft, H.P., 2008. Oxygen groups in coals and alginite-rich kerogen
686 revisited. *International Journal of Coal Geology* 74, 93-113.

687 Petmecky, S., Meier, L., Reiser, H., Littke, R., 1999. High thermal maturity in the Lower Saxony Basin:
688 intrusion or deep burial? *Tectonophysics* 304, 317-344.

689 Pittman, E.D., Lewan, M.D., 1994. *Organic Acids in Geological Processes*. Springer-Verlag Berlin
690 Heidelberg.

691 Robin, P.L., Rouxhet, P.G., 1978. Characterization of kerogens and study of their evolution by infrared
692 spectroscopy: carbonyl and carboxyl groups. *Geochimica et Cosmochimica Acta* 42, 1341-1349.

693 Rullkötter, J., Leythaeuser, D., Horsfield, B., Littke, R., Mann, U., Müller, P.J., Radke, M., Schaefer, R.G.,
694 Schenk, H.J., Schwochau, K., Witte, E.G., Welte, D.H., 1988. Organic matter maturation under the
695 influence of a deep intrusive heat source: A natural experiment for quantitation of hydrocarbon
696 generation and expulsion from a petroleum source rock (Toarcian shale, northern Germany). *Organic*
697 *Geochemistry* 13, 847-856.

698 Sarkhot, D.V., Grunwald, S., Ge, Y., Morgan, C.L.S., 2011. Comparison and detection of total and
699 available soil carbon fractions using visible/near infrared diffuse reflectance spectroscopy. *Geoderma*
700 164, 22-32.

701 Schmidt, F., Elvert, M., Koch, B.P., Witt, M., Hinrichs, K.-U., 2009. Molecular characterization of
702 dissolved organic matter in pore water of continental shelf sediments. *Geochimica Et Cosmochimica*
703 *Acta* 73, 3337-3358.

704 Schmidt, F., Koch, B.P., Witt, M., Hinrichs, K.-U., 2014. Extending the analytical window for water-
705 soluble organic matter in sediments by aqueous Soxhlet extraction. *Geochimica et Cosmochimica*
706 *Acta* 141, 83-96.

707 Schovsbo, N.H., Nielsen, A.T., Klitten, K., Mathiesen, A., Rasmussen, P., 2011. Shale gas investigations
708 in Denmark: Lower Palaeozoic shales on Bornholm. *Geol. Surv. Den. Greenl. Bull.*, 9-12.

709 Seewald, J.S., 2001a. Aqueous geochemistry of low molecular weight hydrocarbons at elevated
710 temperatures and pressures: constraints from mineral buffered laboratory experiments. *Geochimica*
711 *et Cosmochimica Acta* 65, 1641-1664.

712 Seewald, J.S., 2001b. Model for the origin of carboxylic acids in basinal brines. *Geochimica et*
713 *Cosmochimica Acta* 65, 3779-3789.

714 Smith, M.G., Bustin, R.M., 1998. Production and preservation of organic matter during deposition of
715 the Bakken Formation (Late Devonian and Early Mississippian), Williston Basin. *Palaeogeography,*
716 *Palaeoclimatology, Palaeoecology* 142, 185-200.

717 Surdam, R.C., Boese, S.W., Crossey, L.J., 1984. The Chemistry of Secondary Porosity: Part 2. Aspects
718 of Porosity Modification. In: McDonald, D.A. and Surdam, R.C. (eds.), *Clastic Diagenesis*. AAPG
719 *Memoir* 37, 127-149.

720 Surdam, R.C., Jiao, Z.S., MacGowan, D.B., 1993. Redox reactions involving hydrocarbons and mineral
721 oxidants; a mechanism for significant porosity enhancement in sandstones. *AAPG Bulletin* 77, 1509-
722 1518.

723 Tissot, B.P., Welte, D.H., 1984. *Petroleum Formation and Occurrence*. Springer-Verlag, Berlin.

724 Vieth, A., Mangelsdorf, K., Sykes, R., Horsfield, B., 2008. Water extraction of coals – potential for
725 estimating low molecular weight organic acids as carbon feedstock for the deep terrestrial biosphere.
726 *Organic Geochemistry* 39, 985-991.

727 Vu, T.T.A., Horsfield, B., Mahlstedt, N., Schenk, H.J., Kelemen, S.R., Walters, C.C., Kwiatek, P.J., Sykes,
728 R., 2013. The structural evolution of organic matter during maturation of coals and its impact on
729 petroleum potential and feedstock for the deep biosphere. *Organic Geochemistry* 62, 17-27.

730 Vu, T.T.A., Zink, K.G., Mangelsdorf, K., Sykes, R., Wilkes, H., Horsfield, B., 2009. Changes in bulk
731 properties and molecular compositions within New Zealand Coal Band solvent extracts from early
732 diagenetic to catagenetic maturity levels. *Organic Geochemistry* 40, 963-977.

733 Webster, R.L., 1984. *Petroleum source rocks and stratigraphy of Bakken formation in North Dakota*.

734 Weiss, H.M., Wilhelms, A., Mills, N., Scotchmer, J., Hall, P.B., Lind, K., Brekke, T., 2000. NIGOGA - The
735 Norwegian Industry Guide to Organic Geochemical Analyses. Edition 4.0. Available:
736 <http://www.npd.no/engelsk/nigoga/default.htm>.

737 Werner-Zwanziger, U., Lis, G., Mastalerz, M., Schimmelmann, A., 2005. Thermal maturity of type II
738 kerogen from the New Albany Shale assessed by ¹³C CP/MAS NMR. *Solid State Nuclear Magnetic*
739 *Resonance* 27, 140-148.

740 Wilkes, H., Clegg, H., Disko, U., Willsch, H., Horsfield, B., 1998. Fluoren-9-ones and carbazoles in the
741 Posidonia Shale, Hils Syncline, northwest Germany. *Fuel* 77, 657-668.

742 Zinger, A.S., Kravchik, T.E., 1973. Simpler organic acids in groundwater in the Lower Volga Region
743 (genesis and possible use for prospecting for oil). *Doklady Akademii Nauk (Academy of Sciences*
744 *Reports) S.S.S.R.* 202, 218-221.